

Preparation and Characterization of Hydrogels Based on Dehydroabietyl Polyoxyethylene Glycidyl Ether Grafted Hydroxyethyl Chitosans and Their Capability for Loading and Controlled Release of Chloramphenicol

Xujuan Huang,^a Zhenqing Ding,^a Zhaosheng Cai,^{a,*} Ting Wang,^a Xinxin Yang,^b and Shibin Shang^b

Dehydroabietol polyoxyethylene(10) ether (DHA(EO)₁₀H) was reacted with epichlorohydrin (ECH) using BF₃ as catalyst and transformed into DHA(EO)₁₀H-ECH, then dehydrochlorinated in the presence of sodium hydroxide and converted into dehydroabietyl polyoxyethylene(10) glycidyl ether (DHA(EO)₁₀GE). Hydroxyethyl chitosan (HEC) was modified with DHA(EO)₁₀GE, and a series of different DHA(EO)₁₀GE-grafted HECs (DHA(EO)₁₀GE-*g*-HECs) were prepared. Finally, the hydrogels based on DHA(EO)₁₀GE-*g*-HECs were obtained through the reaction between genipin (GE) and DHA(EO)₁₀GE-*g*-HECs. Effects of the grafting degree (DG) of DHA(EO)₁₀GE and the dosage of GE on the gelation ability of mixed solution composed of DHA(EO)₁₀GE-*g*-HECs and GE were investigated, and the behaviors of DHA(EO)₁₀GE-*g*-HEC/GE hydrogels as carriers for loading chloramphenicol (CAP) were studied. It was found that the gelling time of the DHA(EO)₁₀GE-*g*-HEC with high DG was longer than that with low DG, and a higher GE dosage could improve the capability of DHA(EO)₁₀GE-*g*-HEC to form hydrogels. The relation between the cumulative release rate of CAP, which was loaded in DHA(EO)₁₀GE-*g*-HEC/GE gel, and the release times in artificial intestinal fluid could be well described by Boltzmann function. Increasing the DG or decreasing the GE dosage could improve the final cumulative release.

DOI: 10.15376/biores.17.3.4331-4346

Keywords: Hydroxyethyl chitosan; Dehydroabietyl polyoxyethylene glycidyl ether; Modification; Hydrogels; Drug release

Contact information: a: School of Chemistry and Chemical Engineering, Yancheng Institute of Technology, Yancheng 224051 Jiangsu Province, P.R. China; b: Institute of Chemical Industry of Forest Products, Chinese Academy of Forestry, Nanjing 210042 Jiangsu Province, P. R. China;

* Corresponding author: jsyc_czs@163.com

INTRODUCTION

Hydrogels are hydrophilic materials with three-dimensional (3D) crosslinked polymeric network structures that can absorb and retain a significant amount of water without dissolving in it (Drury and Mooney 2003; Piantanida *et al.* 2019). As the ideal materials for the 3D encapsulation of cells, hydrogels have the potential to provide a highly hydrated tissue-like environment. Hydrogels may also incorporate bioactivities, such as growth factors, to mimic the tissue-specific signals. This can influence the embryonic development, proliferation, and even the differentiation of the cells (Peppas *et al.* 2000; McKay *et al.* 2014; Liu *et al.* 2018). Hydrogels could also be utilized as useful devices for drugs delivery, and the release performance of drugs loaded in the hydrogels

could be adjusted by controlling the crosslinked density or using different hydrogels (Dong *et al.* 2016; Zhao *et al.* 2017). Synthetic and natural polymers can be utilized to prepare hydrogels (Marsich *et al.* 2008; Kempaiah and Nie 2014). Hydrogels based on natural polymers possess numerous advantages that make them ideal candidates for biomedical applications (Feng *et al.* 2010; Lai and Shum 2015). The hydrogels based on biopolymers, such as chitosan (CTS), cellulose, and starch, have become important materials for tissue engineering, wound healing, drug loading and controlled release, and cell culture applications (Sacco *et al.* 2014).

CTS is a natural polysaccharide that is obtained by the partial deacetylation of chitin, which is a highly abundant natural polymer composed of N-acetylglucosamine and glucosamine residues (Ravi Kumar 2000; Shariatnia 2019). Due to its biocompatibility, biodegradability, nontoxicity, and ability to be transformed into a cationic polymer through protonation, CTS has been examined and proposed as a biomaterial in the development of controlled and targeted release of drug delivery systems (Supper *et al.* 2014; Zhou *et al.* 2015). Hydroxyethyl chitosan (HEC) is one of the most important derivatives of CTS and can be obtained through the reaction between CTS and a hydroethylating agent (Liang *et al.* 2011). The introduction of hydroxyethyl groups into the sugar chain of CTS can improve its spatial structure, weaken the inter-molecular forces, and increase the water-solubility. This can endow HEC with excellent properties, such as moisturizing, film-forming, and antioxidation, among others (He *et al.* 2017; Wang *et al.* 2017). These excellent properties give HEC the ability to be applied as an antioxidant, a tissue engineering material, a medicine carrier, a medical dressing, and others. HEC and its derivatives have been employed as one of components for preparing hydrogels that can be utilized to load and control the release of drugs (Hou *et al.* 2021).

Gum rosin (GR) is a natural product that is obtained by heating pine oleoresin, which is produced from pine and conifer trees, by vaporizing the volatile liquid terpene components (Wilbon *et al.* 2013). The main component of GR is rosin acids, which are the complex mixture of several compounds, particularly abietic acid and pimaric acid (Sacripante *et al.* 2015). Rosin's excellent biocompatibility and biodegradation features mean that it is safe to use, and hence many of its derivatives have been applied in pharmaceutical fields (Kreps *et al.* 2017; Li *et al.* 2019). Dehydroabietic acid (DHAA) is a carboxylic acid with hydrogenated phenanthrene nucleus and isolated from disproportionated rosin (Sacripante *et al.* 2015). The presence of a phenanthrene nucleus could endow the DHAA with lipophilicity and rigidity (Lei *et al.* 2017), and the presence of carboxyl groups could endow it with reactivity including esterification, salification, and amidation. These properties make DHAA a suitable material for use in different fields, such as in the preparation of surfactants, the synthesis of drugs, and the manufacturing of coatings (Feng *et al.* 2018). Dehydroabietinol (DHA) is a derivative of DHAA, and it is obtained through reducing methyl dehydroabietate or DHAA. Monodehydroabietyl polyethylene glycol(n) ether (DHA(EO)_nH) is an etherifying product of DHA reacted with oxirane, and it could be utilized to prepare dehydroabietyl polyoxyethylene(n) glycidyl ether (DHA(EO)_nGE). Similar to the dehydroabietyl glycidyl ether (DAGE) (Guo *et al.* 2020), the presence of epoxy group could also endow the DHA(EO)_nGE with the ability to react with the water-soluble derivatives of CTS and introduce the phenanthrene nucleus and polyoxyethylene structure into their sugar chain. Meanwhile, because the phenanthrene nucleus is one of the hydrophobic groups with rigidity, and the polyoxyethylene chain is a hydrophilic-lipophilic structure with flexibility (Ito *et al.* 2013; Arslan 2020), the DHA(EO)_nGE-modified water-soluble derivatives of CTS could possess

the capability to aggregate into micelle with large lipophilic core in aqueous solution. The DHA(EO)_nGE-modified water-soluble derivatives of CTS could then be utilized as a special carrier for loading poorly water-soluble drugs and increasing their solubility in physiological conditions without compromising their pharmaceutical performance.

Genipin (GE) is the hydrolyzing product of geniposide, which is isolated from the fruits of Gardenia (Park *et al.* 2002; Nunes *et al.* 2018). It has been widely used as an antiphlogistic and a cholagogue in herbal medicines (Feng *et al.* 2011; Muzzarelli *et al.* 2015). The existence of a recessive glutaraldehyde structure in the GE molecule could endow it with the capability to react with amino groups by nucleophilic addition condensation (Chen *et al.* 2005). The cytotoxicity of GE is approximately 5,000 to 10,000 times less than that of glutaraldehyde (Sung *et al.* 2003), so it has been utilized as a safe crosslinking agent for the fixation of biological tissues. Several animal studies concerned with the biocompatibility of the GE-fixed tissues indicated that its inflammatory reaction was significantly less than that of their glutaraldehyde-fixed counterparts (Hurst 2017; Du *et al.* 2020). With GE as crosslinking agent, CTS aqueous solution (pH between 4.0 and 5.5) and microemulsion composed with Tween 80, Span 20, and isopropyl myristate (IPM), could be transformed into a hydrogel for the extended release of hydrophobic drugs (Delmar and Bianco-Peled 2016). In the past decades, several reports concerned with CTS/GE hydrogels have been published (Wu *et al.* 2014). However, there are few studies about the hydrogels based on HEC, and no works concerned with hydrogels based on rosin-modified HEC have been published thus far. Due to its special structure and good hydrophilic and lipophilic balance, rosin-modified HEC could potentially offer stable capability to load and control the release of both water-soluble drugs and oil-soluble drugs. A series of novel and ecofriendly hydrogels based on DHA(EO)_nGE grafted HECs (DHA(EO)_nGE-g-HECs) with GE as crosslinking agent were prepared in this study, and the properties and capabilities of the hydrogels to load and control the release of chloramphenicol (CAP) were investigated. The detail procedure for preparing drug-loaded hydrogels is shown in Scheme 1.



Scheme 1. Preparation of drug-loaded hydrogels

EXPERIMENTAL

Materials

The DHA (99%) was purchased from Shenzhen Vtolo Industrial Co. (Shenzhen, China). The HEC was prepared according to literature (Wang *et al.* 2019), and its degree of substitution (DS) was 112.4%, as determined by elemental analysis. The sodium

hydroxide (NaOH), potassium hydroxide (KOH), boron trifluoride etherate, and epichlorohydrin (ECH) were purchased from Sinopharm Chemical Reagent Co. (Shanghai, China). The dialysis bags were purchased from Biosharp (Beijing, China). All other chemicals were of reagent grade and were used without purification as received.

Instruments and Equipment

The Fourier transform infrared (FTIR) spectra were recorded with potassium bromide (KBr) pellets on a Nicolet Nexux 670 spectrometer (Thermo Fischer Scientific, Waltham, MA, USA). The liquid samples were referenced against KBr pellets, while the solid samples were referenced against air. The ^1H NMR patterns were obtained at 500.13 MHz with a Bruker DRX-500 spectrometer (Billerica, MA, USA) at 30 ± 0.5 °C, and the samples were dissolved in a 5 mm diameter tube at a concentration of approximately 20 mg/mL with D_2O as solvent.

Preparation of DHA(EO)₁₀H and DHA(EO)₁₀GE

The DHA (143.3 g, 0.50 mol) and KOH (0.86 g) were added into a reaction kettle, which was equipped with an electromagnetic stirrer, a gas conduit, a manometer, a vacuum system, and a temperature measuring device. The air was then drawn out through the vacuum system before the material temperature reached 100 °C. The residual water in the reaction materials was removed by heating under vacuum condition. When the temperature was approximately 140 °C, the vacuum system was stopped and oxirane was imported into the kettle to make the pressure approximately 0.30 MPa. After 220 g of oxirane (5.0 mol) was imported into the kettle, the valve for controlling the import of the oxirane was shut, and the reaction was maintained until the value of manometer became 0 MPa. The reaction material was cooled with water until the temperature of the reaction materials was below 100 °C. The material was then dissolved using toluene, washed with 5% muriatic acid until the pH was approximately 7, and bleached with hydrogen peroxide solution. Finally, the DHA(EO)₁₀H was obtained by recovering toluene and removing the residual water through vacuum distillation.

The DHA(EO)₁₀GE was prepared using a modified method similar to that reported by Guo *et al.* (2020). Briefly, the obtained DHA(EO)₁₀H was dissolved using toluene before metered boron trifluoride etherate was added. Then, metric ECH was added into the reactant dropwise and the temperature of mixture was controlled below 25 °C during the dropping process. After the ECH was mixed completely, the reaction materials were stirred at 65 °C for 4 h. Then, the reaction intermediate, DHA(EO)₁₀H-ECH, was obtained by removing the toluene and unreacted ECH from the reactant using vacuum distillation. An appropriate amount of toluene and 40% of NaOH solution were added into the DHA(EO)₁₀H-ECH and stirred at 35 °C for 5 h. Then the obtained mixture was washed with saturated sodium chloride solution until the pH of the separated aqueous solution was approximately 7. The organic phase was collected and dehydrated using anhydrous sodium sulfate. Finally, the DHA(EO)₁₀GE, an oil-like liquid with light yellow, was obtained by recovering toluene through vacuum distillation.

Synthesis of DHA(EO)₁₀GE-g-HECs

The DHA(EO)₁₀GE-g-HECs were synthesized through the condensation reaction between DHA(EO)₁₀GE and HEC in the presence of NaOH. Briefly, dried HEC (2.16 g, 10 mmol sugar unit) was dispersed in 50 mL of dimethyl sulfoxide (DMSO) at 50 °C. Then, metrological DHA(EO)₁₀GE, which was dissolved in 50 mL of DMSO, and NaOH (4 g)

were added into the reactant in sequence. After the mixture was reacted at 50 °C for 48 h, it was dispersed in 400 mL of ethanol with stirring and then stored at -18 °C for approximately 12 h to ensure the floccule precipitated sufficiently. The floccule was separated from the mixture and then dissolved using 200 mL of distilled water. The pH of the aqueous solution was adjusted to approximately 7, then transferred into dialysis bag and dialyzed against distilled water. After 48 h, the dialyzed solution was concentrated and the remainder was treated using ethanol. The blend was filtered, and the DHA(EO)₁₀GE-g-HEC was obtained by lyophilizing the filter residue under vacuum.

Preparation of DHA(EO)₁₀GE-g-HEC-based Hydrogels

The DHA(EO)₁₀GE-g-HEC aqueous solution (3.5% w/w) and the GE aqueous solution (10 mg/mL) were prepared firstly. Then, the metric DHA(EO)₁₀GE-g-HEC solution was added into an ampoule bottle and mixed with the metric GE solution under stirring. The ampoule bottle was sealed and stored in a 37 ± 0.5 °C water bath after the mixture was transformed into a homogenous phase, and the fluidity of the mixture was observed every 5 min using the inverted bottle method. When the fluidity could not be observed, it meant that the mixture had become the hydrogel and the corresponding time could be regarded as the gelling time.

Preparation of Drug-Loaded Hydrogels and the Release Behavior of Drugs *in vitro*

Metric CAP was added into the solution of DHA(EO)₁₀GE-g-HEC and stirred to ensure it was dispersed sufficiently. The hydrogels were then prepared according to the above, except that the ampoule bottle was stored in the water bath for 36 h. The release of the CAP loaded in the DHA(EO)_nGE-g-HEC-based hydrogels was investigated *in vitro* with phosphate buffered saline (PBS) solution (pH equal to 7.4) as the release medium. The dialysis bag filled with the drug-loaded gel was placed in a conical flask, and 100 mL of PBS solution was added to ensure the dialysis bag was immersed in the release medium. Then, the conical flask was shaken at 37 ± 0.5 °C using a shaker at a speed of 130 revolutions per min. 5 mL of solution was removed from the release medium at a special time, and the other 5 mL of fresh PBS solution was added to keep the total volume of the release medium at 100 mL. The absorbance of the withdrawn liquid was measured at 278 nm and the concentration of CAP in the solution was determined according to the standard curve concerned with the relationship between absorbance and concentration. Finally, Eq. 1 was used to calculate and determine the cumulative release rate of CAP at different times. All the experiments were conducted in triplicate.

$$F_i = \frac{5\sum_1^{i-1} C_n + 100C_i}{\text{Total amount of drug in the hydrogel}} \times 100 \quad (1)$$

In Eq. 1, F_i is the cumulative release rate of drug after $No.i$ sampling (%), C_i is the concentration of CAP in the release medium determined at the time of $No.i$ sampling (mg/mL), 5 was the solution volume of sampling (mL), and 100 was the total volume of the release medium (mL).

RESULTS AND DISCUSSION

Results for the Grafting Degree (DG) of the DHA(EO)₁₀GE-g-HECs

The DG of the different DHA(EO)₁₀GE-g-HECs was determined according to the results of elemental analysis (EA) and calculated using Eq. 2,

$$DG = \frac{7 \times C/N - 48 + 12DD - 12DS}{258} \quad (2)$$

where *C/N* is the mass ratio of the total carbon *versus* total nitrogen of the DHA(EO)₁₀GE-g-HEC samples, *DD* is the degree of deacetylation of the CTS (87.95%), and *DS* is the substitution degree of hydroxyethylation of HEC (112.39%).

Two kinds of DHA(EO)₁₀GE-g-HECs were obtained with the mass ratio of DHA(EO)₁₀GE *versus* sugar unit of HEC. The samples had mass ratios of 1.0 and 2.0, and the results concerned with their elemental analysis can be seen in Table 1.

As shown in Table 1, the increase of the mass ratio of DHA(EO)₁₀GE *versus* sugar unit could result in the increase of DG. The increase of DHA(EO)₁₀GE in the reactant could provide much more opportunity for the reaction between DHA(EO)₁₀GE and HEC, and it was favorable for much more DHA(EO)₁₀GE to graft into the sugar chain.

Table 1. Results of EA of the DHA(EO)₁₀GE-g-HECs and their DG Values

Sample	n(DHA(EO) ₁₀ GE):n(sugar unit)	C Content (%)	N Content (%)	DG (%)
DHA(EO) ₁₀ GE-g-HEC I	1.0:1.0	53.58	4.218	14.72
DHA(EO) ₁₀ GE-g-HEC II	2.0:1.0	54.98	3.739	20.15

Results and Ascription of FTIR, Ultraviolet (UV), and ¹H NMR Analysis

The FTIR spectra of DHA(EO)₁₀H, DHA(EO)₁₀H-ECH, and DHA(EO)₁₀GE are shown in Fig. 1. The FTIR spectra of CTS, HEC, and DHA(EO)₁₀GE-g-HEC are shown in Fig. 2.

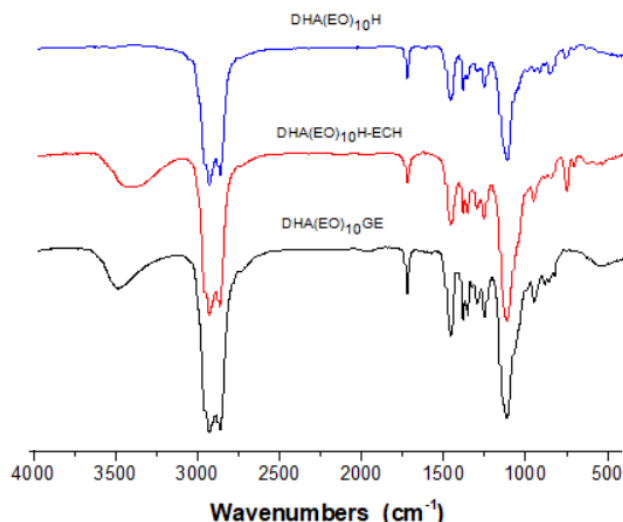


Fig. 1. FTIR spectra of DHA(EO)₁₀H, DHA(EO)₁₀H-ECH, and DHA(EO)₁₀GE

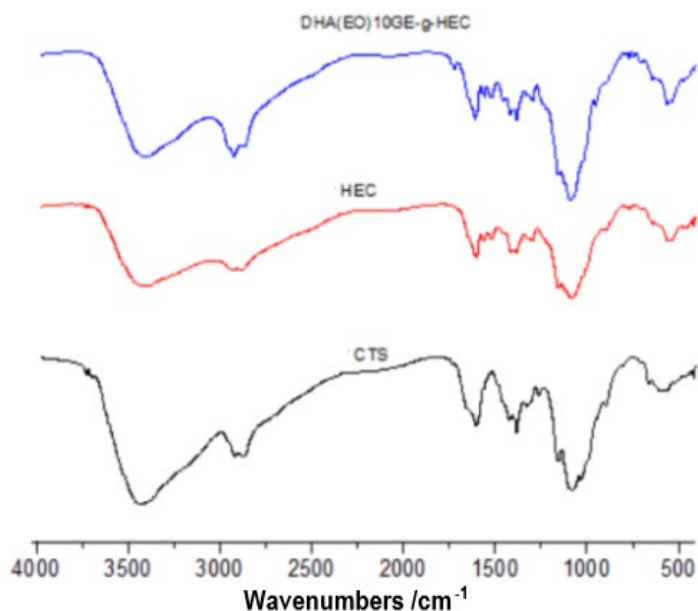


Fig. 2. FTIR spectra of CTS, HEC, and DHA(EO)₁₀GE-g-HEC

In the FTIR spectrum of DHA(EO)₁₀H, the absorption peak at 3490 cm⁻¹ was ascribed to ν_{O-H} of hydroxyl, the peaks at 2937 and 2871 cm⁻¹ were ascribed to ν_{C-H} of methyl and methylene, respectively. The peak at 1109 cm⁻¹ was ascribed to ν_{C-O} of the ether bond, and the peak at 1723 cm⁻¹ was ascribed to $\nu_{C=O}$ of the residual methyl dehydroabietate in DHA(EO)₁₀H. Compared with the FTIR spectrum of DHA(EO)₁₀H, a new peak was seen at 747 cm⁻¹ in that of DHA(EO)₁₀H-ECH, and it was ascribed to ν_{C-Cl} of the C-Cl bond. In addition, the absorption peak concerned with ν_{O-H} of hydroxyl had disappeared in the FTIR spectrum of DHA(EO)₁₀GE.

In the FTIR spectrum of CTS, the broad peak at 3428 cm⁻¹ was ascribed to ν_{O-H} of hydroxyl and ν_{N-H} of amino. The peaks at 2971 and 2924 cm⁻¹ were assigned to ν_{C-H} of CH₂ and CH, respectively. The absorption peaks at 1636 and 1316 cm⁻¹ were ascribed to amide I and III, respectively. The peak at 1384 cm⁻¹ was ascribed to δ_{C-H} of methyl, and the peak at 1156 cm⁻¹ was ascribed to the oxygen bridge. The peaks at 1053 and 1083 cm⁻¹ were attributed to ν_{C-O} of alcohol. In the spectrum of HEC, a strong peak represented δ_{C-H} of CH₂ occurred at 1449 cm⁻¹. A wide strong peak representing ν_{C-O} of primary alcohol occurred at 1070 cm⁻¹ and indicated much more primary hydroxyl existed its structure. The strong peak at 1303 cm⁻¹ was assigned to the ν_{C-N} of secondary amine and indicated some of substitution reactions had happened on the amino group of CTS. Compared with the spectra of CTS and HEC, the intensity of absorption peaks at 2971 and 2924 cm⁻¹ concerned with ν_{C-H} of CH₂ and CH remarkable increased in the FTIR spectrum of DHA(EO)₁₀GE-g-HEC. This indicated that more methyl and methylene were present in the structure of DHA(EO)₁₀GE-g-HEC. Meanwhile, some peaks concerned with the $\nu_{C=C}$ of aromatic ring were observed at 1612, 1562, and 1455 cm⁻¹.

The UV spectra of HEC and DHA(EO)₁₀GE-g-HEC are shown in Fig. 3. The ¹H NMR spectrum of DHA(EO)₁₀GE-g-HEC is shown in Fig. 4.

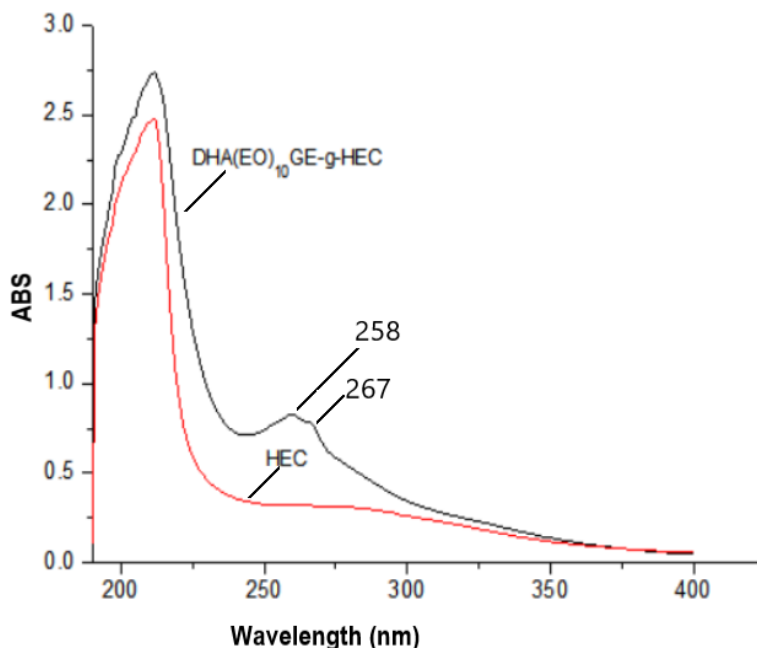


Fig. 3. UV absorption spectra of HEC and DHA(EO)₁₀GE-g-HEC

In the UV absorption spectrum of HEC aqueous solution, an absorption band associated with the C-N bond was seen at approximately 220 nm. Compared the UV absorption spectrum of DA(EO)₁₀GE-g-HEC aqueous solution with that of HEC aqueous solution, it could be seen there existed some differences between them. Other than the absorption band at approximately 220 nm, there were two absorption bands at 258 and 267 nm, which were associated with the aromatic ring structure, in the UV absorption spectrum of DA(EO)₁₀GE-g-HEC. This indicated that the hydrogenated phenanthrene nucleus of DHA was present in the structure of DHA(EO)₁₀GE-g-HEC.

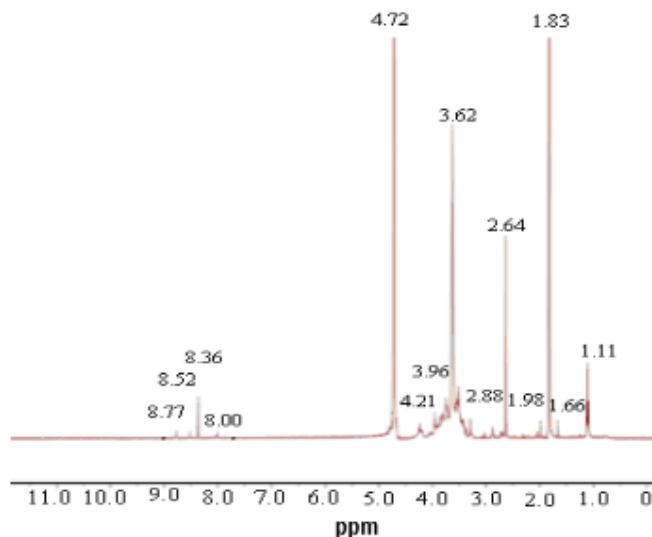


Fig. 4. ¹H NMR spectrum of DHA(EO)₁₀GE-g-HEC

In the ¹H NMR spectrum of DHA(EO)₁₀GE-g-HEC, the peak at 4.21 represented the proton on C1 of sugar unit, and the peak between 3.85 and 4.0 represented the proton

on C5 of modified sugar unit. The peaks at 3.58 to 3.80, 3.40 to 3.58, and 3.0 were associated with the protons on C3, C6, and C2 of the sugar unit, respectively. The peaks at approximately 2.88 and 2.64 represented the H on C4 of sugar unit and that of methylene and methyne of the hydrophenylene ring. The peaks at 8.77, 8.52, 8.36, and 8.02 were ascribed to the H of benzene ring of the hydrogenated phenanthrene nucleus. The strong proton peaks at 1.0 to 1.50 and 1.50 to 2.0 were associated with the proton of methyl and methylene in the polyoxyethylene chain and dehydroabietylalcohol, respectively. The above results indicated the structure of dehydroabietyl polyoxyethylene had been introduced into the sugar chain of HEC.

Gelating Behavior of the DHA(EO)₁₀GE-g-HEC/GE Mixed Solution

The hydrogelation behaviors of the mixed solution composed of different DHA(EO)₁₀GE-g-HECs and GE with various mass ratio are shown in Table 2.

Table 2. Gelating Times of the DA(EO)₁₀GE-g-HEC Aqueous Solution at 37 °C

Sample	V _{DHA(EO)₁₀GE-g-HEC} (mL)	V _{GE} (mL)	Gelling Time (min)
Ia	0.70	0.70	190
Ib	1.0	0.50	255
Ic	0.90	0.30	325
Id	1.0	0	-
IIa	0.70	0.70	310
IIb	1.0	0.50	415
IIc	0.90	0.30	620
IId	1.0	0	-

I: Sample of DHA(EO)₁₀GE-g-HEC with DG of 14.72%; II: Sample of DHA(EO)₁₀GE-g-HEC with DG of 20.15%. The “-” indicates the solution could not transform into gel after 36 h.

The presence of GE and the increase of its mass ratio in the mixed solution were favorable for the DHA(EO)₁₀GE-g-HEC/GE mixed solution forming the hydrogel, and the increase of DG of DHA(EO)₁₀GE-g-HEC resulted in prolonged gelling times of the mixed solution. These results are primarily attributed to the ability of GE to promote the crosslinking among different sugar chains of DHA(EO)₁₀GE-g-HEC. The increase in the DG could decrease the amount of unsubstituted amino groups in the molecular structure of DHA(EO)₁₀GE-g-HECs and decrease its ability to form Schiff-base through nucleophilic addition reaction between GE and unsubstituted aminos.

Release Behavior of CAP Loaded in the DHA(EO)₁₀GE-g-HECs/GE Hydrogel

Effect of the DG and GE usage on the release of drug-loaded in the hydrogels

The drug-loaded gels were prepared by using 10 mg/mL of GE and 3.5% of different DHA(EO)₁₀GE-g-HEC aqueous solution in various ratios. The cumulative release rate of the drug was investigated with 0.320% of CAP content in the hydrogels, and the results are shown in Fig. 5.

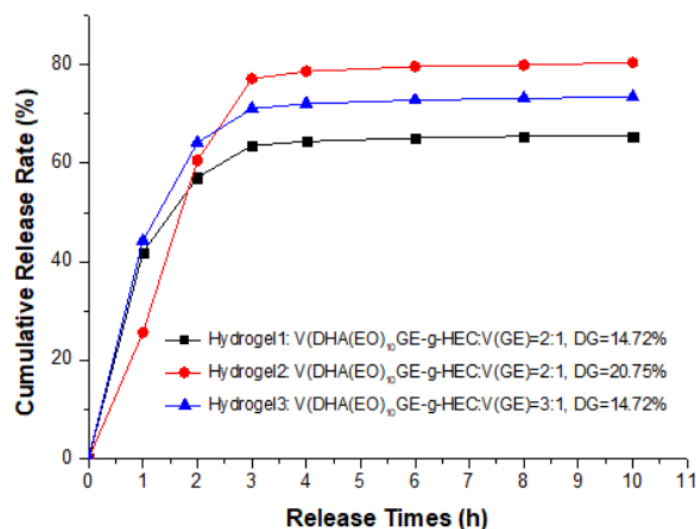


Fig. 5. Relation of the release times and the cumulative release rate of the drug-loaded hydrogels

The experimental results indicated that the increase of DG of DHA(EO)₁₀GE-g-HEC was unfavorable for the initial release of CAP from hydrogels but favorable for improving its cumulative release rate. An increased GE content in the mixed solution could result in the decrease of cumulative release rate of CAP from the hydrogels. The higher DG meant that a more hydrophobic hydrophenylene ring existed in the molecular structure of DHA(EO)₁₀GE-g-HEC and could cause more initial resistance for the polar medium to penetrate the hydrogels. However, the higher DG also meant that there were fewer unsubstituted amino groups in the molecular structure of DHA(EO)₁₀GE-g-HEC, which resulted in the formation of DHA(EO)₁₀GE-based hydrogels with low crosslinking density and was favorable for the diffusion of more drugs from the hydrogels into the release solution. The increased GE mass ratio in the mixed solution was favorable for the formation of DA(EO)₁₀GE-g-HEC-based hydrogels with a high crosslinking density. This could result in the increased resistance of drug diffusion from the hydrogels to the medium and the decreased ability of the medium to penetrate the hydrogels.

Release kinetics of drug-loaded in different hydrogels

OriginPro 8.5.1 software (Originlab Co., Northampton, MA, USA) was utilized to investigate the release kinetics of the CAP loaded in the DA(EO)₁₀GE-g-HEC/GE hydrogels. The relationships between the cumulative release rate of CAP and the release times for different drug-loaded hydrogels were fitted using different nonlinear function. The fitted results can be seen in Fig. 6, Fig. 7, Fig. 8, and Table 3.

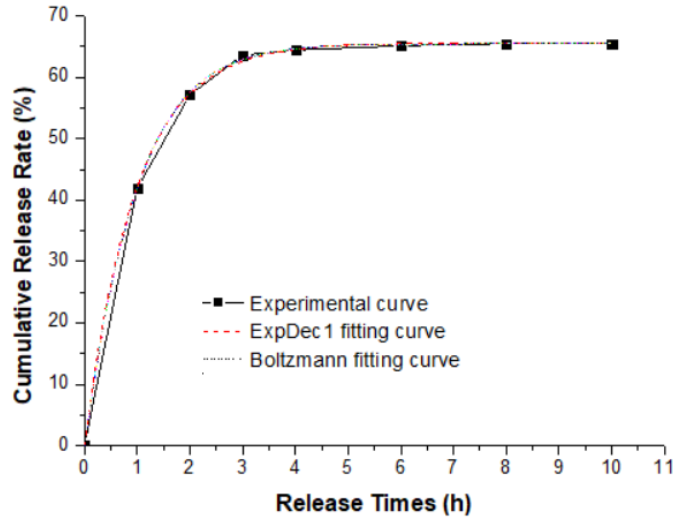


Fig. 6. The fitting curve of the release behavior of the CAP from hydrogel 1

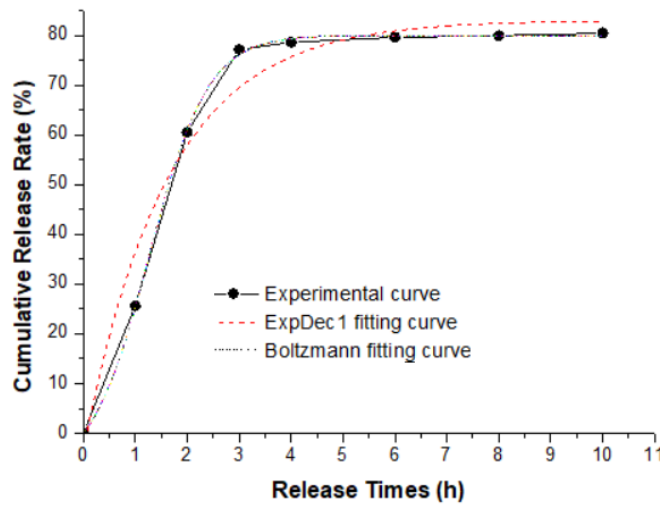


Fig. 7. The fitting curve of the release behavior of the CAP from hydrogel 2

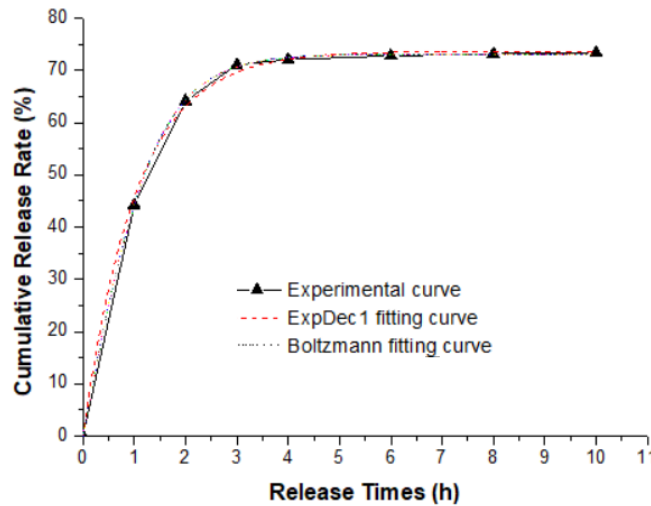


Fig. 8. Fitting curve of the release behavior of the CAP from hydrogel 3

The fitting results data indicated that the Boltzmann function ($y=A_2+(A_1-A_2)/(1+\exp((x-x_0)/dx))$) could be utilized to describe the relationship between the cumulative release rate of CAP, which was loaded in the DHA(EO)₁₀GE-g-HEC/GE hydrogels, and the release times in the PBS buffer solution with coefficients of determination higher than 0.999. Meanwhile, the ExpDec1 function ($y=A_1*\exp(-x/T_1)+y_0$) could also be utilized to describe the relationship between the cumulative release rate of CAP, which was loaded in the hydrogel obtained composed of DHA(EO)₁₀GE-g-HEC (DG was 14.72%) and GE, and release times excellently. However, when the ExpDec1 function was utilized to describe the relationship between the cumulative drug release rate and the release time for the hydrogel obtained from DHA(EO)₁₀GE-g-HEC (DG was 20.15%) crosslinked with GE, the coefficient of determination was lower than 0.96. The fitting results showed the release behavior of CAP that loaded in the hydrogels, which was obtained through the crosslinking reaction between GE and DHA(EO)₁₀GE-g-HEC with low DG, was in accordance with the first-order kinetics equation. However, the release behavior of CAP loaded in the hydrogels that was obtained from GE and DHA(EO)₁₀GE-g-HEC with high DG, was approximately in accordance with the first-order kinetics equation.

Table 3. The Fitting Functions for Describing the Relationship between Release Times and Cumulative Release Rate for Different Drug-Loaded Hydrogels and their Coefficients of Determination

Hydrogel Sample	Fitting Function	coefficient of determination
Hydrogel 1	$F = -65.68134 \times \exp(-1.02973t) + 65.61714$	0.99953
	$F = 65.46377 - 260.13986 / (1 + \exp(1.13852 \times (t + 1.40913)))$	0.9996
Hydrogel 2	$F = -86.64533 \times \exp(-t/1.61829) + 83.04387$	0.95426
	$F = 80.02709 - 88.32926 / (1 + \exp(1.77535 \times (t - 1.27134)))$	0.9994
Hydrogel 3	$F = -73.97387 \times \exp(-t/1.02993) + 73.67559$	0.99818
	$F = 73.11953 - 163.5847 / (1 + \exp(1.32674 \times (t + 0.16049)))$	0.99981

F: Cumulative release rate of CAP (%); t: Release time (h).

CONCLUSIONS

1. The dehydroabietyl polyoxyethylene(10) glycidyl ether grafted hydroxyethyl chitosans (DA(EO)₁₀GE-g-HECs), as one of derivatives of chitosan (CTS)-containing phenanthrene nucleus and polyoxyethylene structure, could be prepared by grafting modification of water-soluble hydroxyethyl chitosan (HEC) with dehydroabietyl polyoxyethylene(10) glycidyl ether (DA(EO)₁₀GE) as a grafting agent.
2. When the genipin (GE) was utilized as a crosslinking agent, the aqueous solution of DA(EO)₁₀GE-g-HECs could be transformed into hydrogels. The increased GE or the decreased grafting degree (DG) could result in lower gelling times of mixed aqueous solution composed of DA(EO)₁₀GE-g-HECs and GE.
3. The DA(EO)₁₀GE-g-HECs/GE hydrogels could be utilized as one of carriers for loading CAP, and the relationship between the cumulative release rate of CAP loaded in the DHA(EO)₁₀GE-g-HEC/GE hydrogels and the release times in the PBS buffer solution could be described using Boltzmann function ($y=A_2+(A_1-A_2)/(1+\exp((x-x_0)/dx))$) with high coefficients of determination.
4. The release behavior of the chloramphenicol (CAP) loaded in the hydrogels that were obtained through the crosslinking reaction between the GE and the DHA(EO)₁₀GE-g-HECs with low DG was in good accordance with the first-order kinetics equation.

ACKNOWLEDGEMENTS

The authors gratefully acknowledge the support of the National Natural Science Foundation of China (Grant No. 32071706) and the Key Laboratory of Biomass Energy and Material of Jiangsu Province (Grant No. JSBEM201909) for funding. The authors are also thankful for the support of the Key and Open Laboratory on Forest Chemical Engineering, SFA and Yancheng Teachers University for assistance with the analysis.

REFERENCES CITED

- Arslan, M. (2020). "Fabrication and reversible disulfide functionalization of PEGylated chitosan-based hydrogels: Platforms for selective immobilization and release of thiol-containing molecules," *European Polymer Journal* 126, 109543. DOI: 10.1016/j.eurpolymj.2020.109543
- Chen, H., Ouyang, W., Lawuyi, B., Martoni, C., and Prakash, S. (2005). "Reaction of chitosan with genipin and its fluorogenic attributes for potential microcapsule membrane characterization," *Journal of Biomedical Materials Research. Part A* 75A(4), 917-927. DOI: 10.1002/jbm.a.30492
- Delmar, K., and Bianco-Peled, H. (2016). "Composite chitosan hydrogels for extended release of hydrophobic drugs," *Carbohydrate Polymers* 136, 570-580. DOI: 10.1016/j.carbpol.2015.09.072
- Dong, R., Zhao, X., Guo, B., and Ma, P. X. (2016). "Self-healing conductive injectable hydrogels with antibacterial activity as cell delivery carrier for cardiac cell therapy," *ACS Applied Materials and Interfaces* 8(27), 17138-17150. DOI:

- 10.1021/acsami.6b04911
- Drury, J. L., and Mooney, D. J. (2003). "Hydrogels for tissue engineering: Scaffold design variables and applications," *Biomaterials* 24, 4337-4351. DOI: 10.1016/S0142-9612(03)00340-5
- Du, J. R., Hsu, L. H., Xiao, E. S., Guo, X., Zhang, Y., and Feng, X. (2020). "Using genipin as a "green" crosslinker to fabricate chitosan membranes for pervaporative dehydration of isopropanol," *Separation and Purification Technology* 244, article no. 116843. DOI: 10.1016/j.seppur.2020.116843
- Feng, X., Lv, F., Liu, L., Tang, H., Xing, C., Yang, Q., and Wang, S. (2010). "Conjugated polymer nanoparticles for drug delivery and imaging," *ACS Applied Materials and Interfaces* 2(8), 2429-2435. DOI: 10.1021/am100435k
- Feng, Q., Cao, H.-l., Xu, W., Li, X.-r., Ren, Y.-q., and Du, L.-f. (2011). "Apoptosis induced by genipin in human leukemia K562 cells: Involvement of c-Jun N-terminal kinase in G₂/M arrest," *Acta Pharmacologica Sinica* 32, 519-527. DOI: 10.1038/aps.2010.158
- Feng, L., Xie, D., Song, B., Zhang, J., Pei, X., and Cui, Z. (2018). "Aggregate evolution in aqueous solutions of a Gemini surfactant derived from dehydroabiatic acid," *Soft Matter* 14(7), 1210-1218. DOI: 10.1039/C7SM02173A
- Guo, W., Cai, Z., Xu, Q., Sun, K., Huang, X., and Cao, Z. (2020). "Synthesis and properties of dehydroabietyl glycidyl ether grafted hydroxypropyl chitosan," *BioResources* 15(2), 4110-4123. DOI: 10.15376/biores.15.2.4110-4123
- He, M., Han, B., Jiang, Z., Yang, Y., Peng, Y., and Liu, "Synthesis of a chitosan-based photo-sensitive hydrogel and its biocompatibility and biodegradability," *Carbohydrate Polymers* 166, 228-235. DOI: 10.1016/j.carbpol.2017.02.072
- Hou, G., Sun, T., Qian, J., Zhang, Y., Guo, M., Xu, W., Wang, J., and Suo, A. (2021). "Hydroxyethyl chitosan hydrogels for enhancing breast cancer cell tumorigenesis," *International Journal of Biological Macromolecules* 184, 768-775. DOI: 10.1016/j.ijbiomac.2021.06.110
- Hurst, G. A. (2017). "Green and smart: Hydrogels to facilitate independent practical learning," *Journal of Chemical Education* 94(11), 1766-1771. DOI: 10.1021/acs.jchemed.7b00235
- Ito, T., Yoshida, C., and Murakami, Y. (2013). "Design of novel sheet shaped chitosan hydrogel for wound healing: A hybrid biomaterial consisting of both PEG-grafted chitosan and crosslinkable polymeric micelles acting as drug containers," *Materials Science and Engineering: C* 33(7), 3697-3703. DOI: 10.1016/j.msec.2013.04.056
- Kempaiah, R., and Nie, Z. (2014). "From nature to synthetic systems: Shape transformation in soft materials," *Journal of Materials Chemistry B* 2(17), 2357-2368. DOI: 10.1039/C3TB21462A
- Kreps, F., Burčová, Z., Jablonský, M., Ház, A., Frečer, V., Kyselka, J., Schmidt, Š., Šurina, I., and Filip, V. (2017). "Bioresource of antioxidant and potential medicinal compounds from waste biomass of spruce," *ACS Sustainable Chemistry and Engineering* 5(9), 8161-8170. DOI: 10.1021/acssuschemeng.7b01816
- Lai, W.-F., and Shum, H. C. (2015). "Hypromellose-graft-chitosan and its polyelectrolyte complex as novel systems for sustained drug delivery," *ACS Applied Materials and Interfaces* 7(19), 10501-10510. DOI: 10.1021/acsami.5b01984
- Lei, L., Xie, D., Song, B., Jiang, J., Pei, X., and Cui, Z. (2017). "Photoresponsive foams generated by a rigid surfactant derived from dehydroabiatic acid," *Langmuir* 33(32), 7908-7916. DOI: 10.1021/acs.langmuir.7b00934

- Li, Z., Yang, X., Liu, H., Yang, X., Shan, Y., Xu, X., Shang, S., and Song, Z. (2019). "Dual-functional antimicrobial coating based on a quaternary ammonium salt from rosin acid with *in vitro* and *in vivo* antimicrobial and antifouling properties," *Chemical Engineering Journal* 374, 564-575. DOI: 10.1016/j.cej.2019.05.208
- Liang, Y., Liu, W., Han, B., Yang, C., Ma, Q., Zhao, W., Rong, M., and Li, H. (2011). "Fabrication and characters of a corneal endothelial cells scaffold based on chitosan," *Journal of Materials Science: Materials in Medicine* 22(1), 175-183. DOI: 10.1007/s10856-010-4190-6
- Liu, Q., Dong, Z., Ding, Z., Hu, Z., Yu, D., Hu, Y., Abidi, N., and Li, W. (2018). "Electroresponsive homogeneous polyelectrolyte complex hydrogels from naturally derived polysaccharides," *ACS Sustainable Chemistry and Engineering* 6(5), 7052-7063. DOI: 10.1021/acssuschemeng.8b00921
- Marsich, E., Borgogna, M., Donati, I., Mozetic, P., Strand, B. L., Salvador, S. G., Vittur, F., and Paoletti, S. (2008). "Alginate/lactose-modified chitosan hydrogels: A bioactive biomaterial for chondrocyte encapsulation," *Journal of Biomedical Materials Research. Part A* 84(2), 364-376. DOI: 10.1002/jbm.a.31307
- McKay, C. A., Pomrenke, R. D., McLane, J. S., Schaub, N. J., DeSimone, E. K., Ligon, L. A., and Gilbert, R. J. (2014). "An injectable, calcium responsive composite hydrogel for the treatment of acute spinal cord injury," *ACS Applied Materials and Interfaces* 6(3), 1424-1438. DOI: 10.1021/am4027423
- Muzzarelli, R. A. A., El Mehtedi, M., Bottegoni, C., Aquili, A., and Gigante A. (2015). "Genipin-crosslinked chitosan gels for tissue engineering and regeneration of cartilage and bone," *Marine Drugs* 13(12), 7314-7338. DOI: 10.3390/md13127068
- Nunes, C., Coimbra, M. A., and Ferreira, P. (2018). "Tailoring functional chitosan-based composites for food applications," *The Chemical Record* 18(7-8), 1138-1149. DOI: 10.1002/tcr.201700112
- Park, J.-E., Lee, J.-Y., Kim, H.-G., Hahn, T.-R., and Paik, Y.-S. (2002). "Isolation and characterization of water-soluble intermediates of blue pigments transformed from geniposide of *Gardenia jasminoides*," *Journal of Agricultural and Food Chemistry* 50(22), 6511-6514. DOI: 10.1021/jf020499b
- Peppas, N. A., Bures, P., Leobandung, W., and Ichikawa, H. (2000). "Hydrogels in pharmaceutical formulations," *European Journal of Pharmaceutics and Biopharmaceutics* 50(1), 27-46. DOI: 10.1016/S0939-6411(00)00090-4
- Piantanida, E., Alonci, G., Bertucci, A., and De Cola, L. (2019). "Design of nanocomposite injectable hydrogels for minimally invasive surgery," *Accounts of Chemical Research* 52(8), 2101-2112. DOI: 10.1021/acs.accounts.9b00114
- Ravi Kumar, M. N. V. (2000). "A review of chitin and chitosan applications," *Reactive and Functional Polymers* 46(1), 1-27. DOI: 10.1016/S1381-5148(00)00038-9
- Sacco, P., Borgogna, M., Travan, A., Marsich, E., Paoletti, S., Asaro, F., Grassi, M., and Donati, I. (2014). "Polysaccharide-based networks from homogeneous chitosan tripolyphosphate hydrogels: Synthesis and characterization," *Biomacromolecules* 15(9), 3396-3405. DOI: 10.1021/bm500909n
- Sacripante, G. G., Zhou, K., and Farooque, M. (2015). "Sustainable polyester resins derived from rosins," *Macromolecules* 48(19), 6876-6881. DOI: 10.1021/acs.macromol.5b01462
- Shariatnia, Z. (2019). "Pharmaceutical applications of chitosan," *Advances in Colloid and Interface Science* 263, 131-194. DOI: 10.1016/j.cis.2018.11.008
- Sung, H.-W., Chang, W.-H., Ma, C.-Y., and Lee, M.-H. (2003). "Crosslinking of

- biological tissues using genipin and/or carbodiimide,” *Journal of Biomedical Materials Research. Part A* 64A(3), 427-438. DOI: 10.1002/jbm.a.10346
- Supper, S., Anton, N., Seidel, N., Riemenschmitter, M., Curdy, C., and Vandamme, T. (2014). “Thermosensitive chitosan/glycerophosphate-based hydrogel and its derivatives in pharmaceutical and biomedical applications,” *Expert Opinion on Drug Delivery* 11(2), 249-267. DOI: 10.1517/17425247.2014.867326
- Wang, Y., Qian, J., Zhao, N., Liu, T., Xu, W., and Suo, A. (2017). “Novel hydroxyethyl chitosan/cellulose scaffolds with bubble-like porous structure for bone tissue engineering,” *Carbohydrate Polymers* 167, 44-51. DOI: 10.1016/j.carbpol.2017.03.030
- Wang, T., Cai, Z.-s., Zhang, T.-t., Li, M., Fang, G.-g., and Zhu, X.-m. (2019). “Dehydroabietyl glycidyl ether grafted hydroxyethyl chitosan: Synthesis, characterization and physicochemical properties,” *Tenside Surfactants Detergents* 56(3), 252-259. DOI: 10.3139/113.110618
- Wilbon, P. A., Chu, F., and Tang C. (2013). “Progress in renewable polymers from natural terpenes, terpenoids, and rosin,” *Macromolecular Rapid Communications* 34(1), 8-37. DOI: 10.1002/marc.201200513
- Wu, F., Meng, G., He, J., Wu, Y., Wu, F., and Gu, Z. (2014). “Antibiotic-loaded chitosan hydrogel with superior dual functions: Antibacterial efficacy and osteoblastic cell responses,” *ACS Applied Materials and Interfaces* 6(13), 10005-10013. DOI: 10.1021/am502537k
- Zhao, L., Niu, L., Liang, H., Tan, H., Liu, C., and Zhu, F. (2017). “pH and glucose dual-responsive injectable hydrogels with insulin and fibroblasts as bioactive dressings for diabetic wound healing,” *ACS Applied Materials and Interfaces* 9(43), 37563-37574. DOI: 10.1021/acsami.7b09395
- Zhou, H. Y., Jiang, L. J., Cao, P. P., Li, J. B., and Chen, X. G. (2015). “Glycerophosphate-based chitosan thermosensitive hydrogels and their biomedical applications,” *Carbohydrate Polymers* 117, 524-536. DOI: 10.1016/j.carbpol.2014.09.094

Article submitted: March 10, 2022; Peer review completed: May 22, 2022; Revisions accepted: May 25, 2022; Published: May 27, 2022.
DOI: 10.15376/biores.17.3.4331-4346